Electronic Supplementary Material (ESI) for ChemComm.

Supporting Information for

Modulation of proton conductivity in coordination polymer mixed glasses

Chonwarin Thanaphatkosol,[a] Nattapol Ma,[b] Kotoha Kageyama,[b] Teerat Watcharatpong,[a] Thanakorn Tiyawarakul,[a] Kanokwan Kongpatpanich *[a] and Satoshi Horike *[abc]

[a] Department of Materials Science and Engineering, School of Molecular Science and Engineering, Vidyasirimedhi Institute of Science and Technology, Rayong, 21210, Thailand

[b] Department of Synthetic Chemistry and Biological Chemistry, Graduate School of Engineering, Kyoto University, Katsura, Nishikyo-ku, Kyoto 615-8510, Japan

[c] Institute for Integrated Cell-Material Sciences-VISTEC Research Center, Institute for Advanced Study, Kyoto University, Yoshida-Honmachi, Sakyo-ku, Kyoto 606-8501, Japan

*Email: horike@icems.kyoto-u.ac.jp (S.H)

Table of Contents

1. Experimental section

1.1 Materials.

All chemicals were reagent grade and used without any further purification. Zinc oxide (ZnO) nanopowder (< 100 nm particle size, 99.99% trace metals basis) was purchased from Sigma-Aldrich. Imidazole (Im) was purchased from Nacalai Tesque, Inc. Benzimidazole (BIm) and phosphoric acid (H_3PO_4, 85% in H_2O) were purchased from Tokyo Chemical Industry Co., Ltd.

1.2 Synthesis of $[Zn(HPO_4)(H_2PO_4)](H_2Im)_2$ (ZnPIm).

ZnPIm was synthesized via a reported method.[1] Zinc oxide (81 mg, 1 mmol), imidazole (136 mg, 2 mmol), ethanol (500 µL), and phosphoric acid (205 µL, 3 mmol) were added to a mortar and ground for 30 minutes. The obtained white precipitate was filtered and washed with ethanol three times. The product was dried at 80 °C in the oven and evacuated overnight to get the dried sample.

1.3 Synthesis of $[Zn_3(H_2PO_4)_6(H_2O)_3](HBIm)$ (ZnPBIm-H_2O).

ZnPBIm-H_2O was synthesized via a reported method.[2] Zinc oxide (243 mg, 3 mmol), benzimidazole (118 mg, 1 mmol), and phosphoric acid (85% in H_2O, 402 µL, 6 mmol) were loaded into a Teflon jar with a steel-cored 15 mm Teflon ball. The mixture was ground for 60 min in a Retch MM400 grinder mill operating at 25 Hz. The obtained powder was then evacuated at 30 °C overnight. An anhydrous phase (ZnPBIm) was obtained by heating under vacuum at 80 °C for 12 h.

1.4 Material characterizations. Powder X-ray diffraction (PXRD) patterns were collected using a Bruker D8ADCANCE with CuKα anode (λ = 1.5405 Å). Thermalgravimetric analysis (TGA) and differential thermal analysis (DTA) results were collected using a Rigaku Thermo plus TG 8122 apparatus with a heating rate of 10 °C min^{-1} under flowing N_2. Pt TGA pans were used to avoid any side reactions. Differential Scanning Calorimetry (DSC) was collected using Perkin Elmer model-lab system-8500 under N_2 atmosphere (Pt crucible, 10 K min^{-1}). All samples were dried under vacuum before each measurement to avoid the contribution from dehydration. The impedance measurements were performed using an Autolab PGSTAT302N plus FRA32M module over the frequency range of 1 Hz – 1 MHz with an input voltage amplitude of 30 mV in a current range of 1 mA. Samples were filled in a liquid state and cooled down to room temperature (melt-quenching). Crystalline sample (ca. 50 mg) was pressed at 500 kgf for 2 min using 5 mm die. The pellet was sandwiched between two gold electrodes. All samples were measured under N_2 atmosphere. Collected data were analysed using Autolab software via equivalent circuit fitting. Scanning electron microscope (SEM) images were taken using a JEOL JSM-7610F after Pt plasma-chemical vapour deposition. Dynamic mechanical analysis and viscosity measurement were evaluated via a rotational parallel-plate rheometer (Discovery Hybrid Rheometer HR20 - TA instruments) under N_2 flow. IR spectra were obtained using a Bruker ALPHA II FT-IR spectrometer with a Universal ATR accessory under N_2. X-ray total scattering was collected at the BL04B2 beamline at the Super Photon ring-8 GeV (SPring-8, Hyogo, Japan) with four CdTe and two Ge detectors covering the Q range up to 25 $Å^{-1}$ (61.377 keV; λ = 0.2020 Å). Each sample was filled in a Lindemann glass capillary with a diameter of 2 mm and sealed inside an Ar-filled glove box. The collected scattering data was applied absorption, background, and Compton scattering corrections then normalised to give the Faber–Ziman total structure factor S(Q). The pair distribution function (PDF) was calculated by Fourier transforming the S(Q) with a Lorch

modification function.[3-5] For extended X-ray absorption fine-structure spectroscopy, each sample was mixed with boron nitride and pressed into pellets with a diameter of 10 mm (0.5 mm thick) and sealed inside an Ar-filled glove box. The synchrotron X-ray absorption spectra in the energy region of the Fe K-edge were collected in transmission mode on the BL01B1 beamline at the Super Photon ring-8 GeV (SPring-8, Hyogo, Japan). Fourier transformation was *k*3-weighted in the *k* range of 3.0 to 14 $Å^{-1}$. The data processing and fitting were performed with Athena and Arthemis software, respectively. N_2 adsorption isotherms were obtained using BELSORP-miniX, MicrotracBEL Crop. 300 mg of samples were pretreated for 24 h at 70 °C before the actual measurements.

2. Supplementary figures and tables

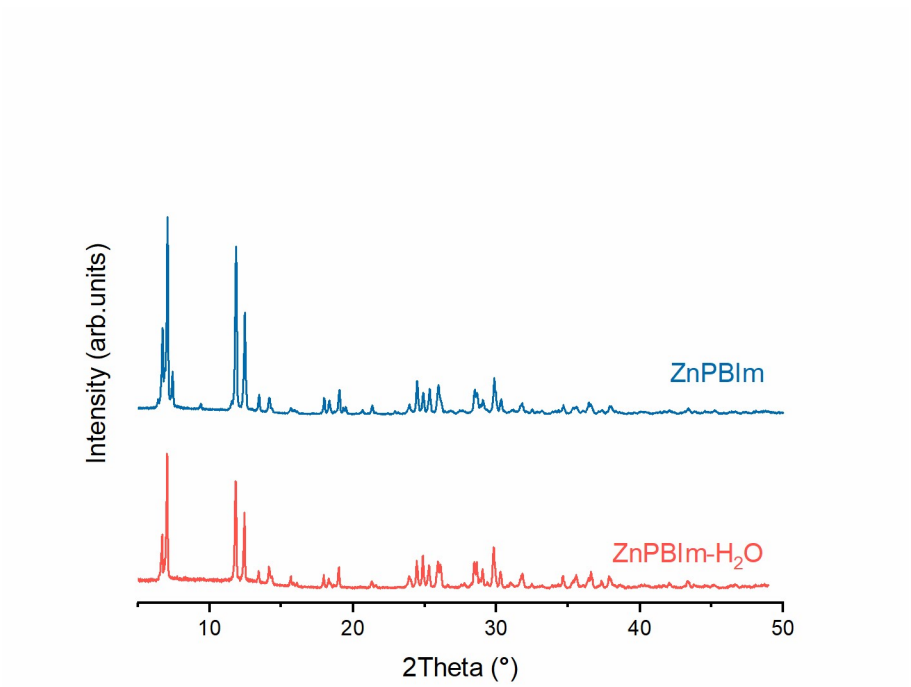

Fig. S1 PXRD of **ZnPBIm** and **ZnPBIm-H_2O**.

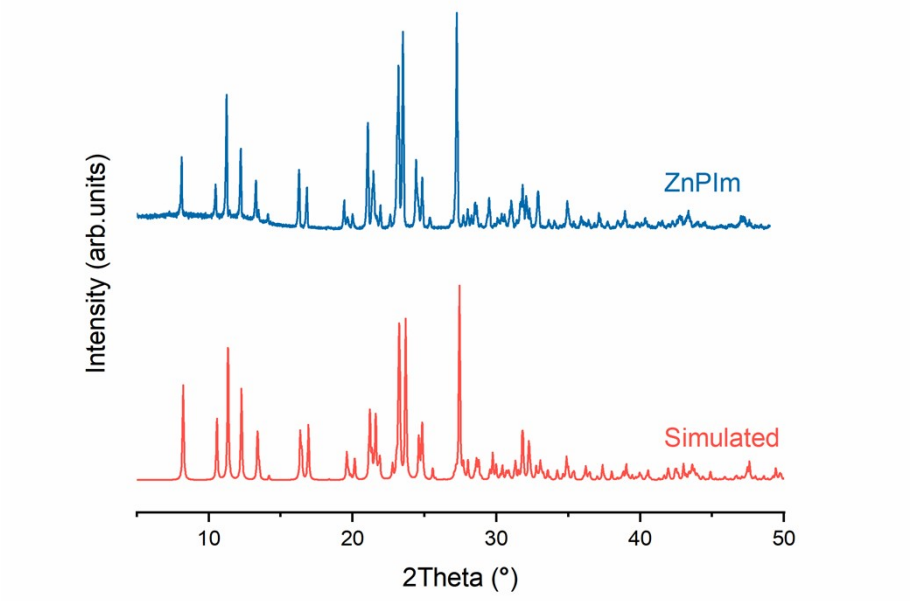

Fig. S2 PXRD of **ZnPIm** (blue) and simulated pattern from crystal structure (red).

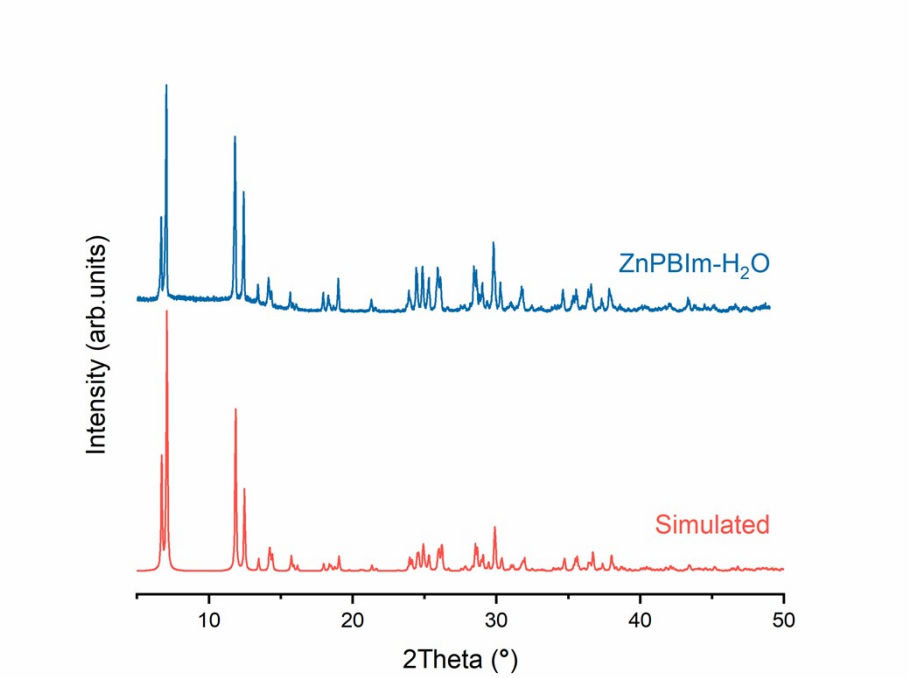

Fig. S3 PXRD of **ZnPBIm-H_2O** (blue) and simulated pattern from crystal structure (red).

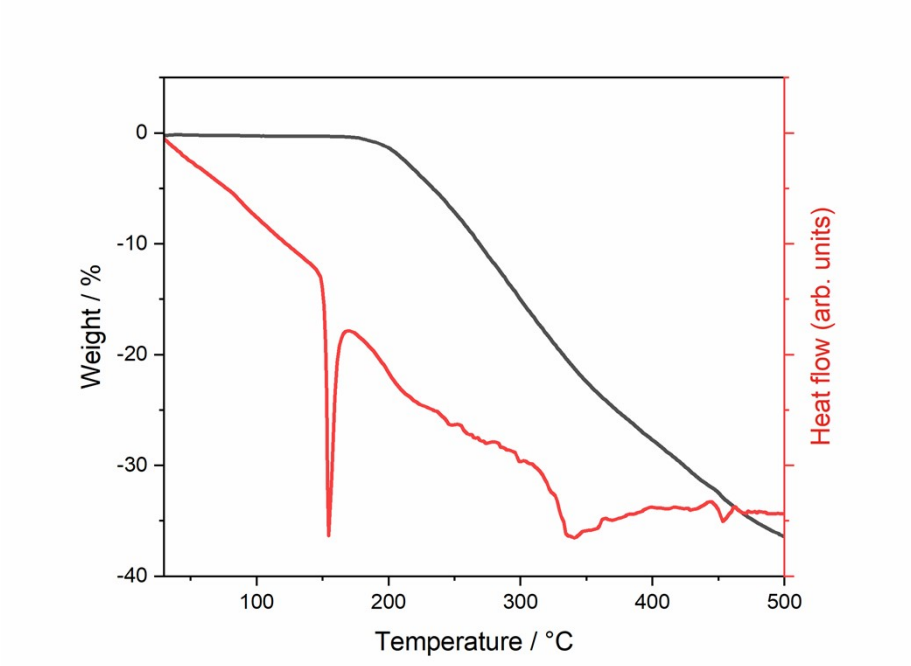

Fig. S4 TGA (black) and DTA (red) of **ZnPIm** under N_2 flow.

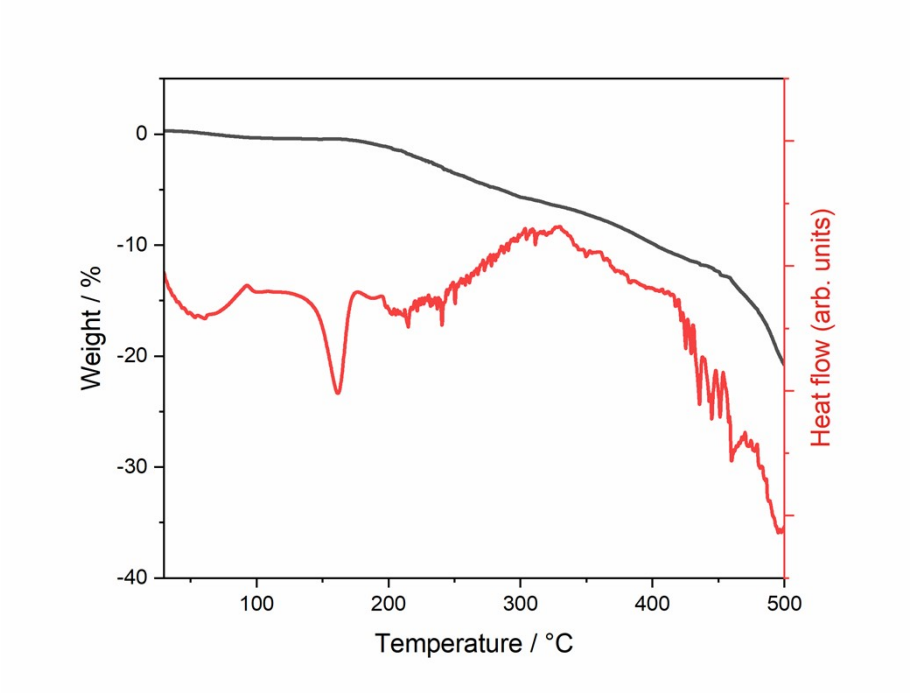

Fig. S5 TGA (black) and DTA (red) of **ZnPBIm** under N_2 flow.

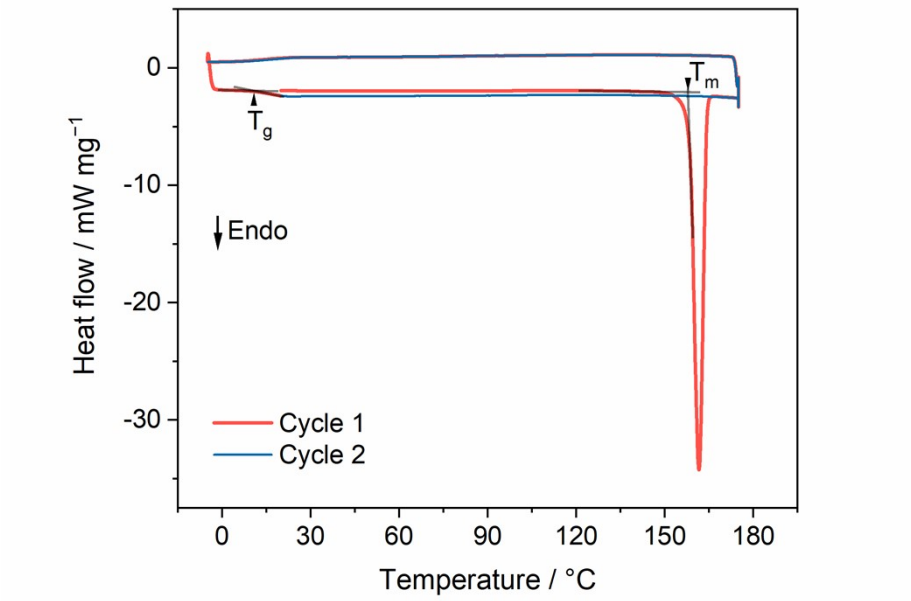

Fig. S6 DSC of **ZnPIm** under N_2 flow. Blue curves represent the first heating and cooling cycles, while red curves display the second cycles.

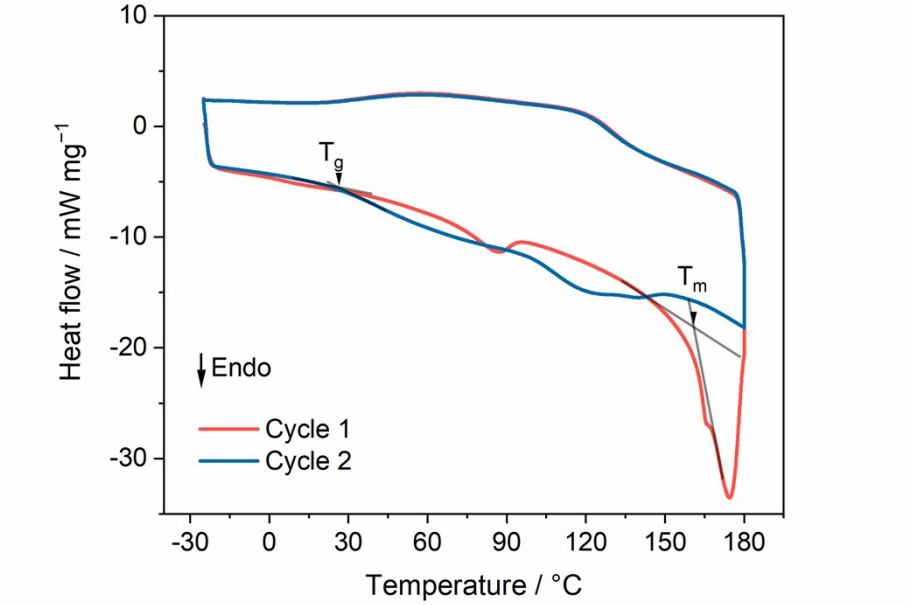

Fig. S7 DSC of **ZnPBIm** under N_2 flow. Blue curves represent the first heating and cooling cycles, while red curves display the second cycles.

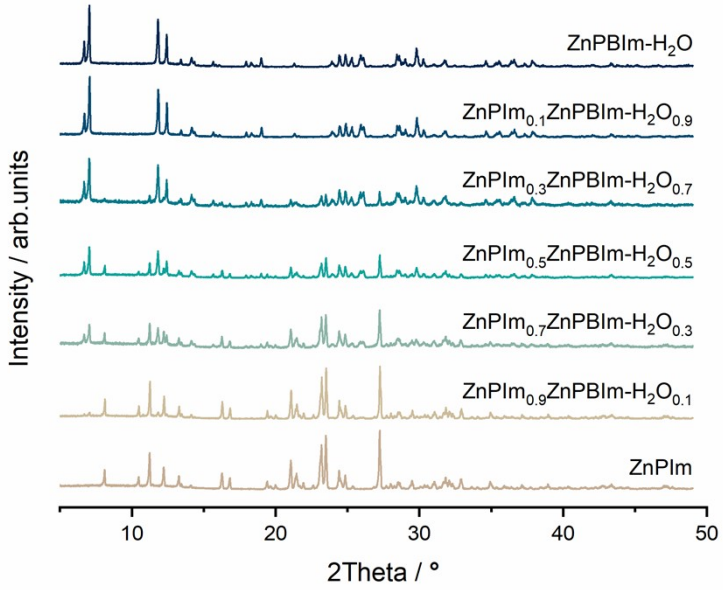

Fig. S8 Powder X-ray diffraction (PXRD) patterns of **ZnPIm**, **ZnPBIm-H_2O**, and **$ZnPIm_{1-x}$ZnPBIm-H_2O_x** mixtures.

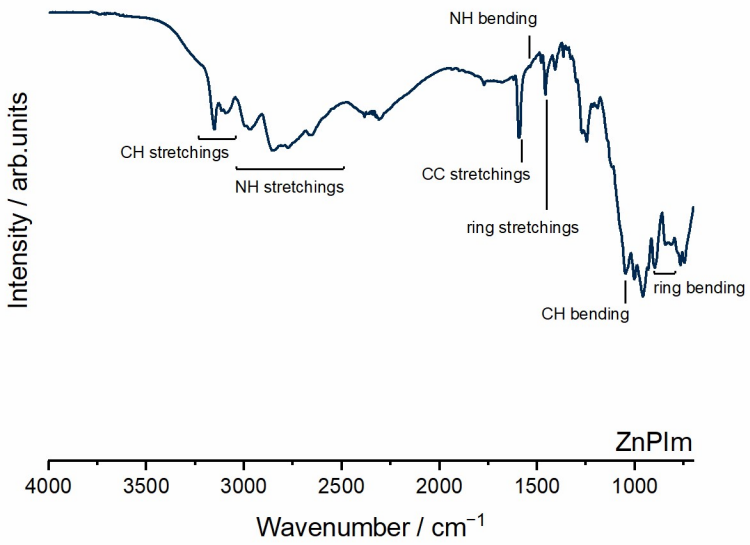

Fig. S9 FTIR spectra of **ZnPIm** and imidazolium peaks labelling. Assignments are based on ref 6, 7.

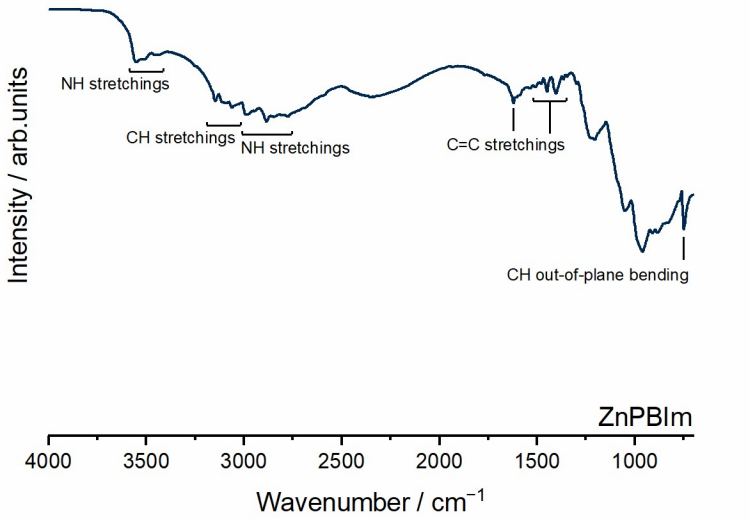

Fig. S10 FTIR spectra of **ZnPBIm** and benzimidazole peaks labelling. Assignments are based on ref 8, 9.

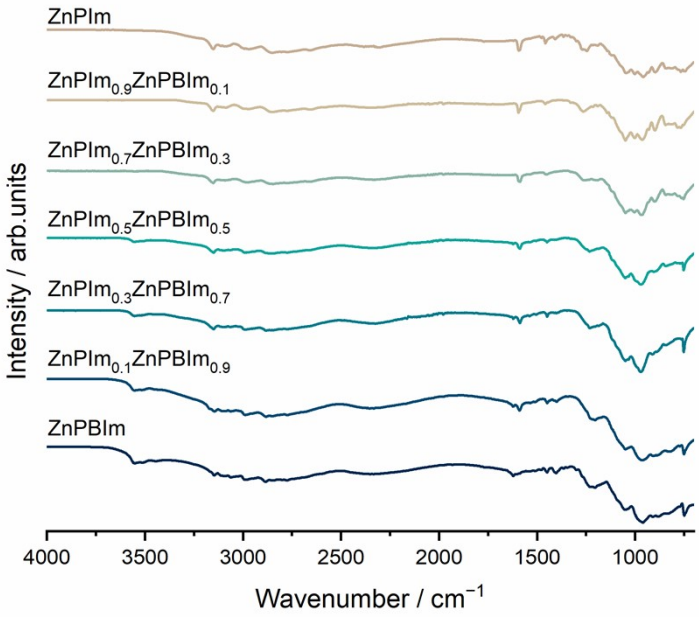

Fig. S11 FTIR spectra of **$ZnPIm_{1-x}ZnPBIm_x$** where *x* = 0, 0.1, 0.3, 0.5, 0.7, 0.9, 1.0.

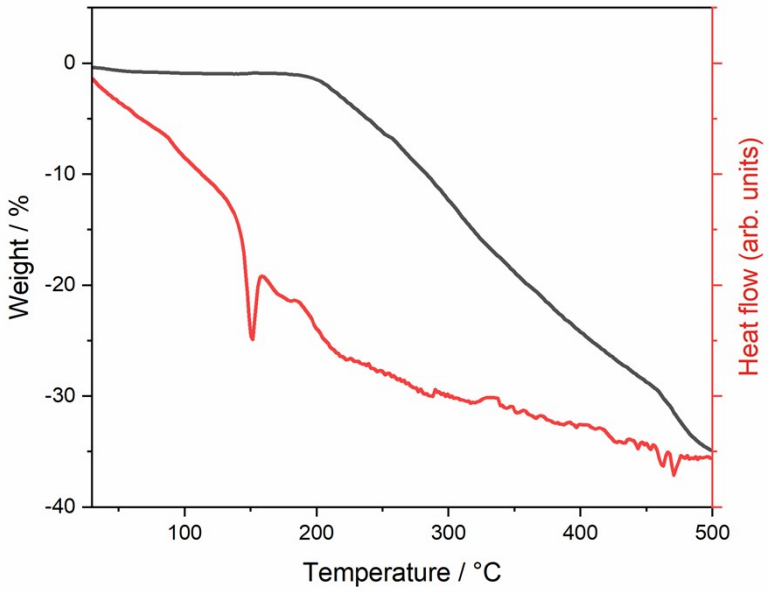

Fig. S12 TGA (black) and DTA (red) of **$ZnPIm_{0.9}ZnPBIm_{0.1}$** under N_2 flow.

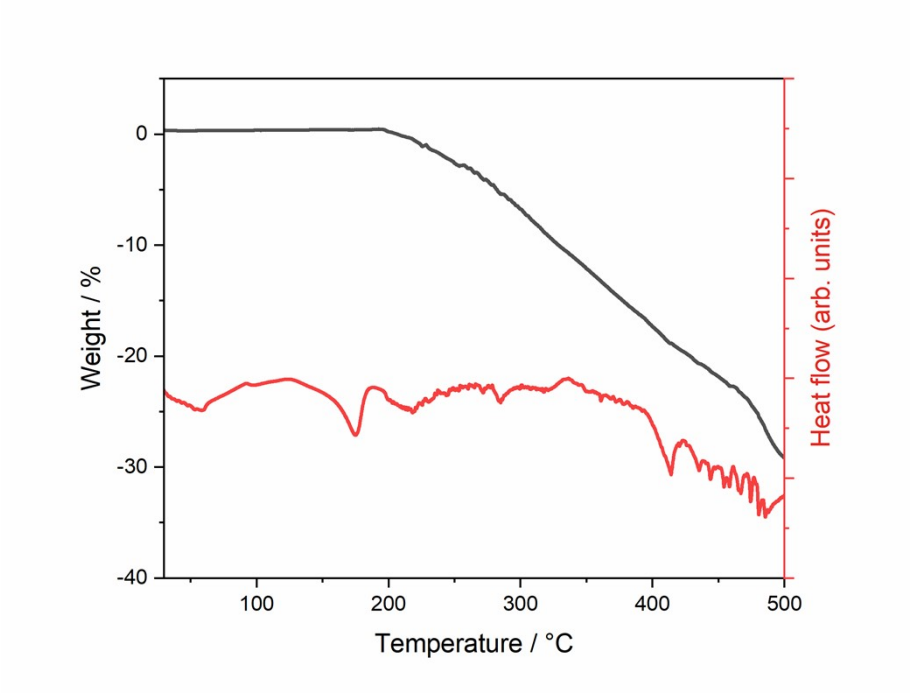

Fig. S13 TGA (black) and DTA (red) of **$ZnPIm_{0.7}ZnPBIm_{0.3}$** under N_2 flow.

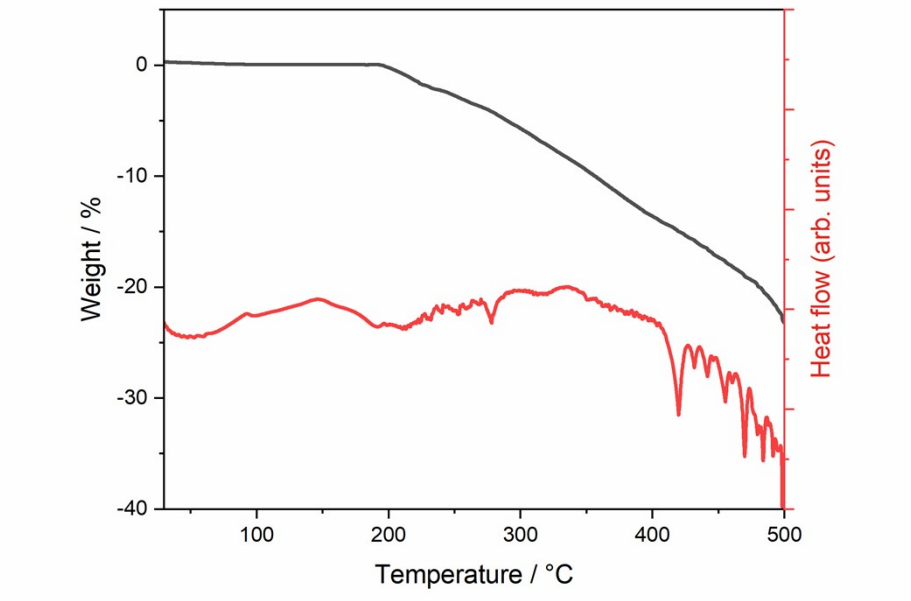

Fig. S14 TGA (black) and DTA (red) of **$ZnPIm_{0.5}ZnPBIm_{0.5}$** under N_2 flow.

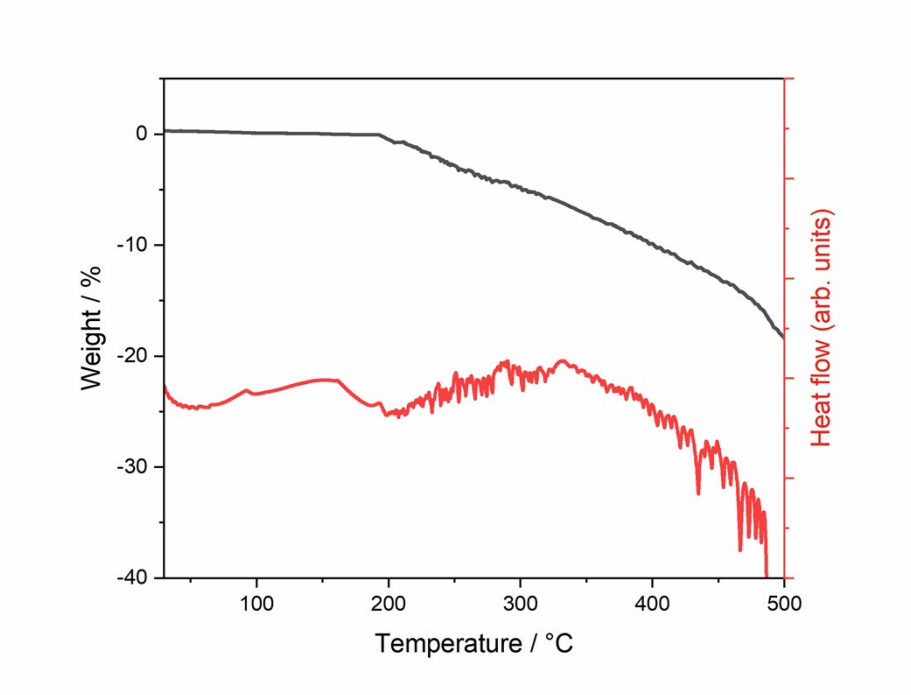

Fig. S15 TGA (black) and DTA (red) of **$ZnPIm_{0.3}ZnPBIm_{0.7}$** under N_2 flow.

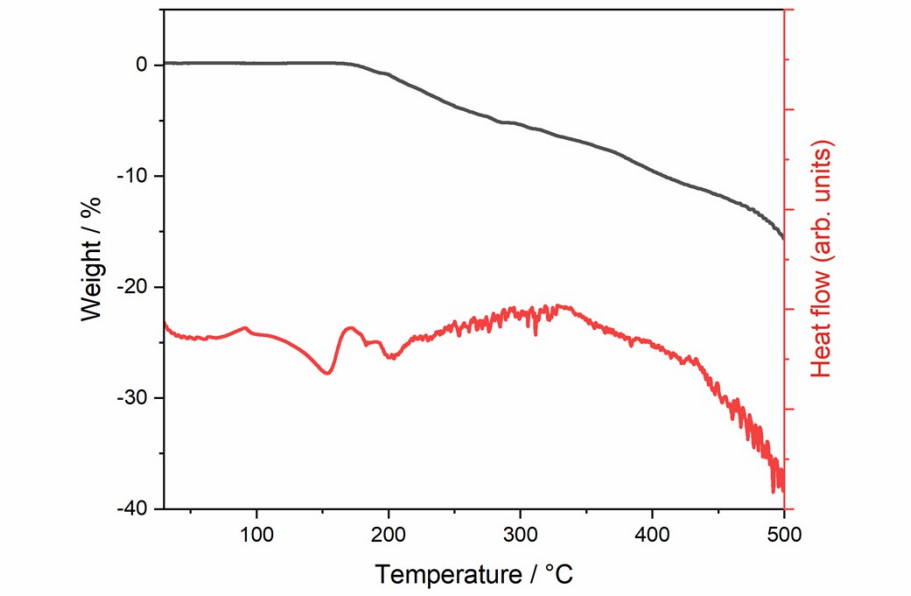

Fig. S16 TGA (black) and DTA (red) of **$ZnPIm_{0.1}ZnPBIm_{0.9}$** under N_2 flow.

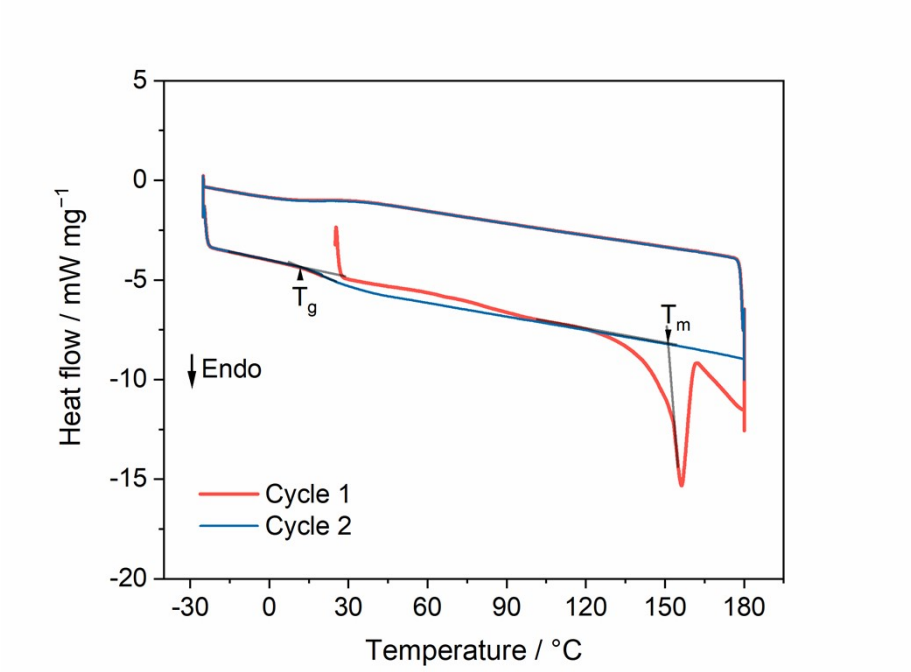

Fig. S17 DSC of **$ZnPIm_{0.9}ZnPBIm_{0.1}$** under N_2 flow. Blue curves represent the first heating and cooling cycles, while red curves display the second cycles.

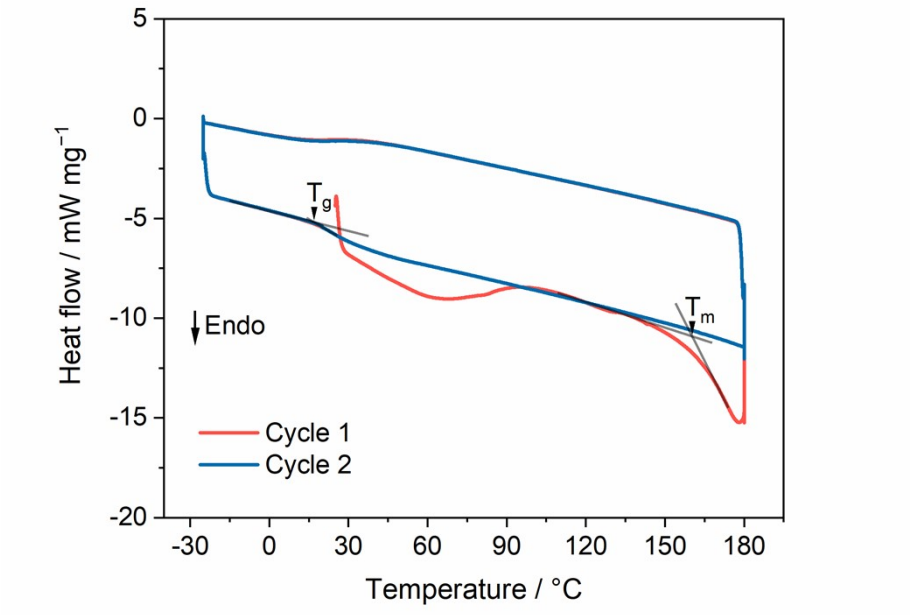

Fig. S18 DSC of **$ZnPIm_{0.7}ZnPBIm_{0.3}$** under N_2 flow. Blue curves represent the first heating and cooling cycles, while red curves display the second cycles.

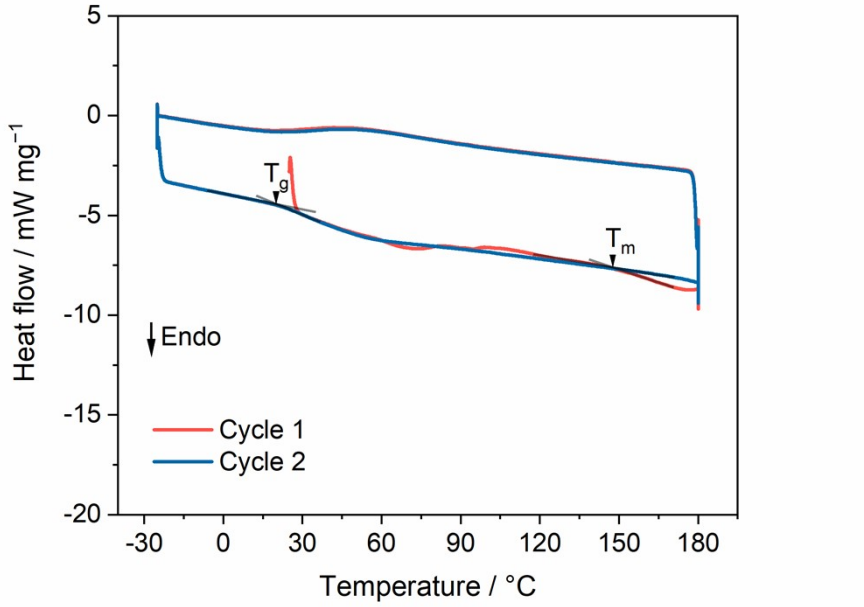

Fig. S19 DSC of **ZnPIm$_{0.5}$ZnPBIm$_{0.5}$** under N_2 flow. Blue curves represent the first heating and cooling cycles, while red curves display the second cycles.

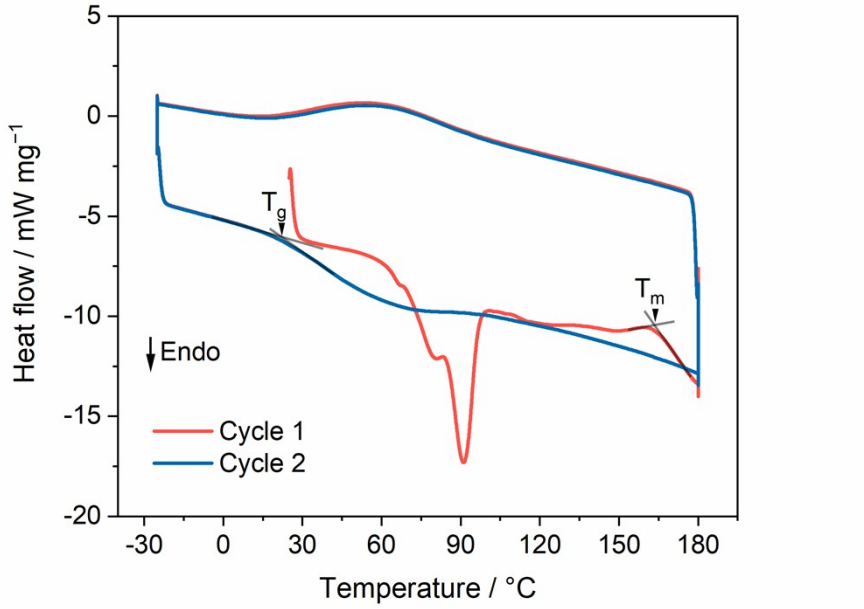

Fig. S20 DSC of **$ZnPIm_{0.3}ZnPBIm_{0.7}$** under N_2 flow. Blue curves represent the first heating and cooling cycles, while red curves display the second cycles.

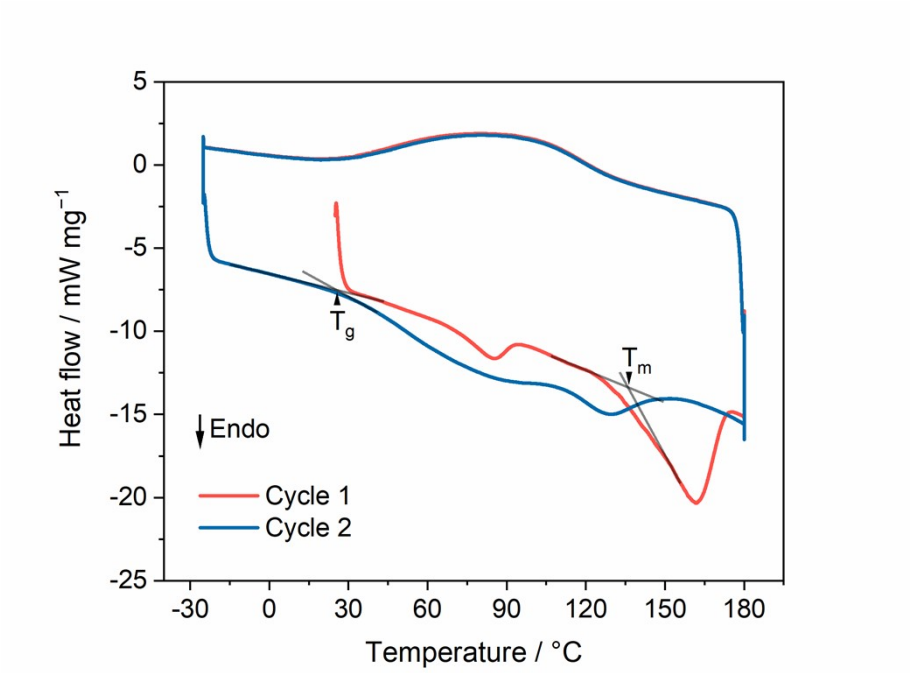

Fig. S21 DSC of **$ZnPIm_{0.1}ZnPBIm_{0.9}$** under N_2 flow. Blue curves represent the first heating and cooling cycles, while red curves display the second cycles.

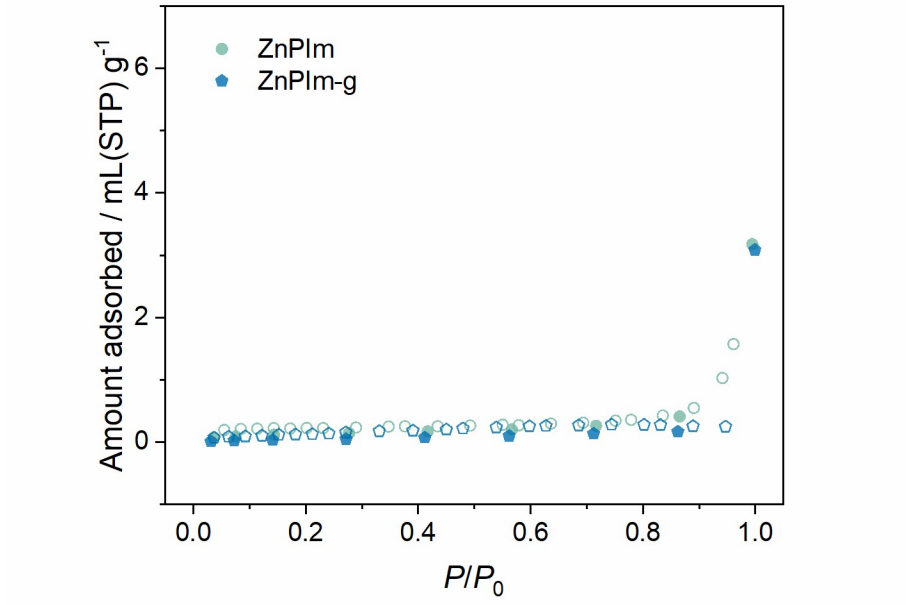

Fig. S22 N_2 adsorption isotherms at 77 K of **ZnPIm** and **ZnPIm-g**. Adsorption and desorption processes are represented by Filled and hollow symbols, respectively.

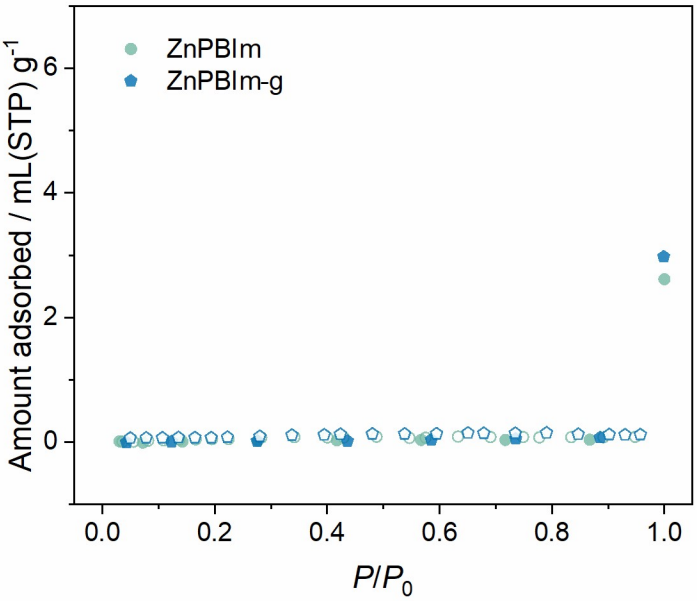

Fig. S23 N_2 adsorption isotherms at 77 K of **ZnPBIm** and **ZnPBIm-g**. Adsorption and desorption processes are represented by Filled and hollow symbols, respectively.

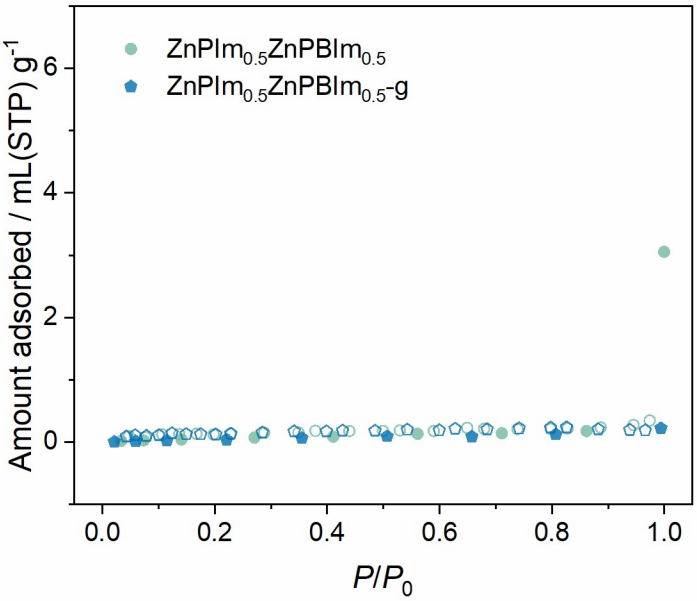

Fig. S24 N_2 adsorption isotherms at 77 K of **$ZnPIm_{0.5}ZnPBIm_{0.5}$** and **$ZnPIm_{0.5}ZnPBIm_{0.5}$-g**. Adsorption and desorption processes are represented by Filled and hollow symbols, respectively.

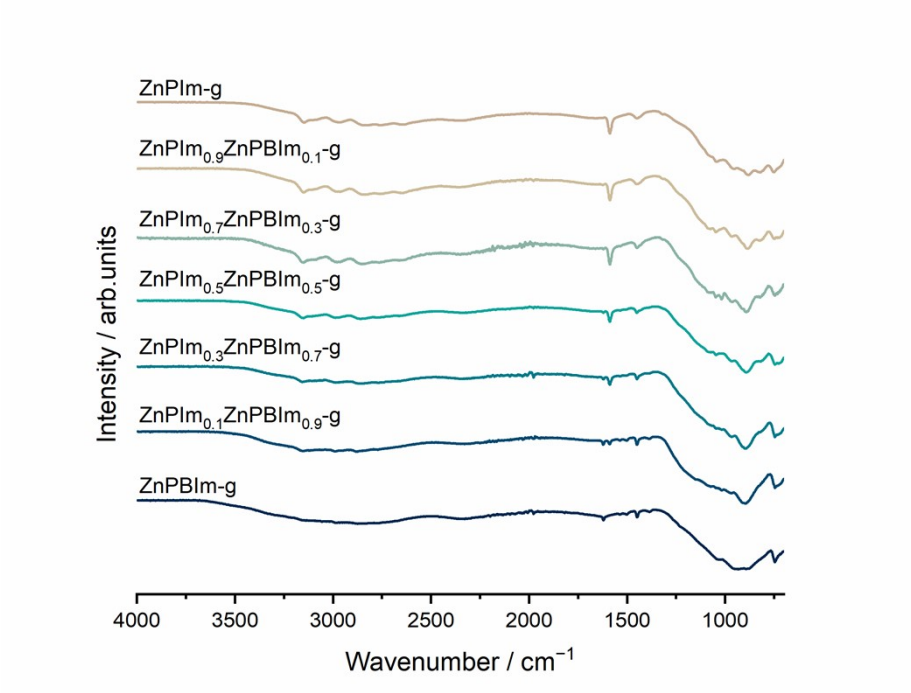

Fig. S25 FTIR spectra of **$ZnPIm_{1-x}ZnPBIm_x$-g** where x = 0, 0.1, 0.3, 0.5, 0.7, 0.9, 1.0.

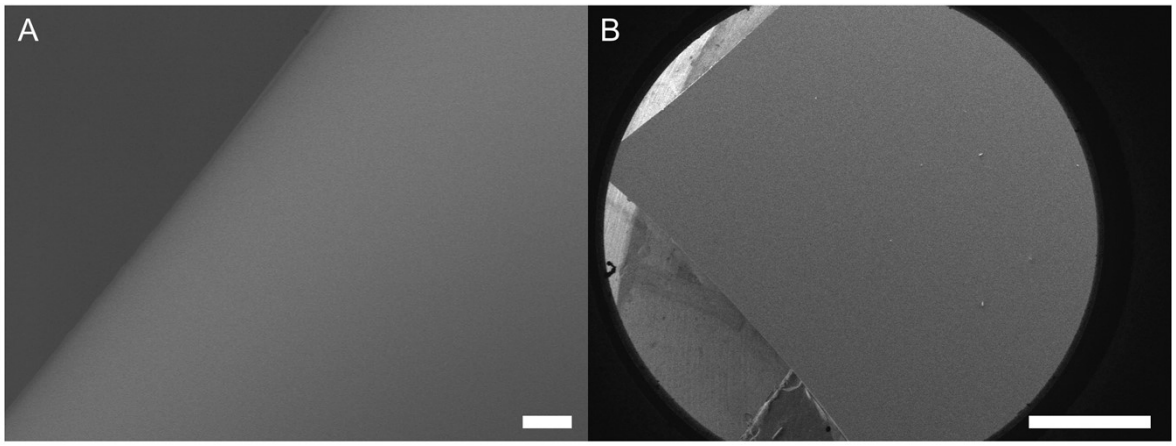

Fig. S26 SEM images of **$ZnPIm_{0.9}ZnPBIm_{0.1}$-g** with (A) x1000 magnification and (B) x25 magnification. Scale bars of (A) 10 µm and (B) 1 mm.

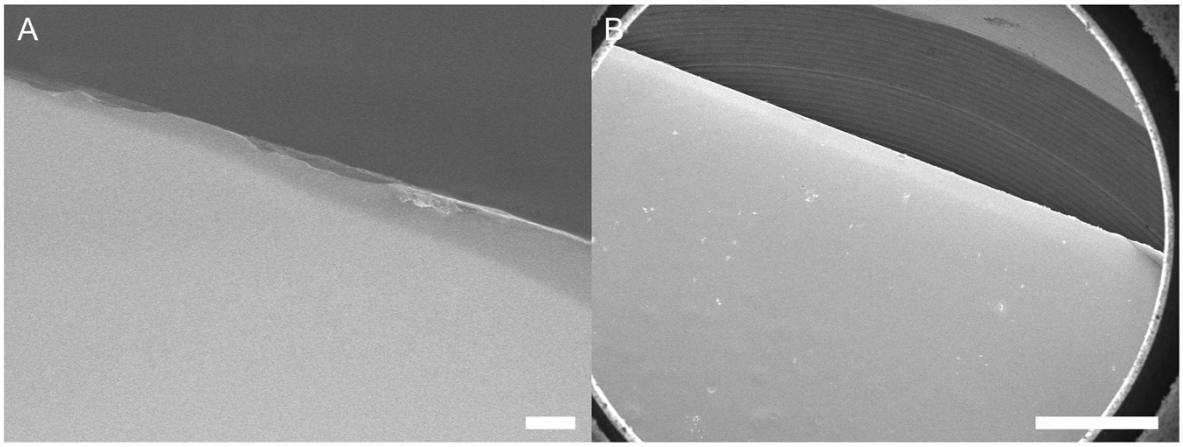

Fig. S27 SEM images of **ZnPIm$_{0.1}$ZnPBIm$_{0.9}$-g** with (A) x1000 magnification and (B) x25 magnification. Scale bars of (A) 10 μm and (B) 1 mm.

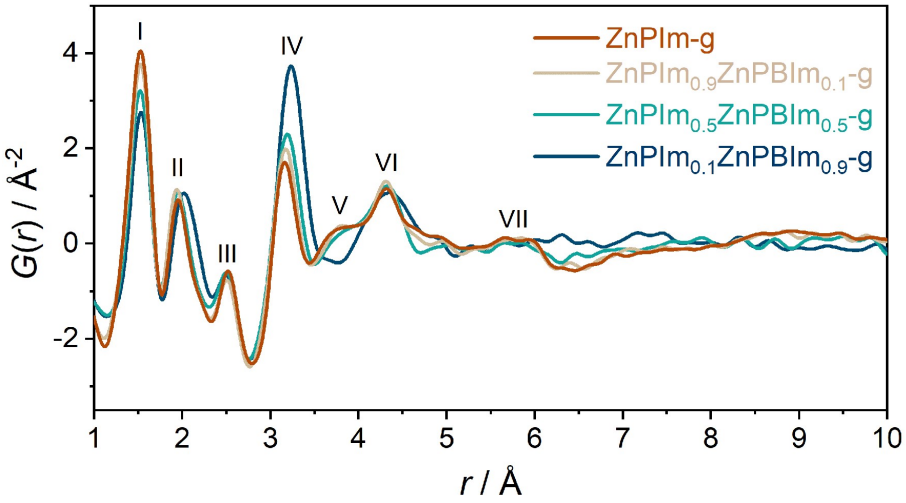

Fig. S28 Pair distribution function (PDF) and PDF peak assignment of **ZnPIm-g** and **ZnPIm$_{1-x}$ZnPBIm$_x$-g** (x = 0.1, 0.5, 0.9).

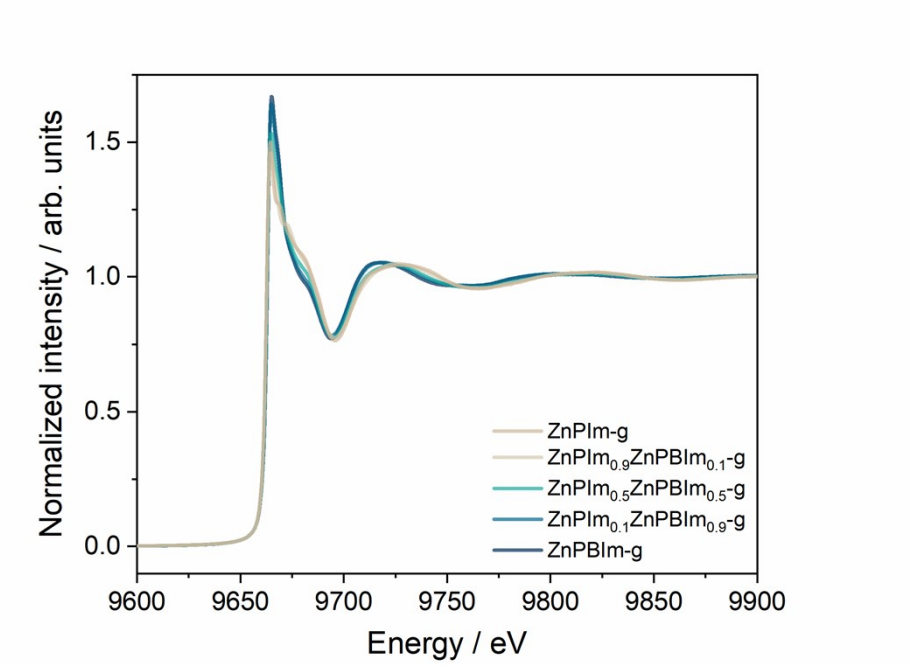

Fig. S29 Normalized X-ray absorption spectroscopy (XAS) spectra of **$ZnPIm_{1-x}ZnPBIm_x$-g** where x = 0, 0.1, 0.5, 0.9, and 1.0.

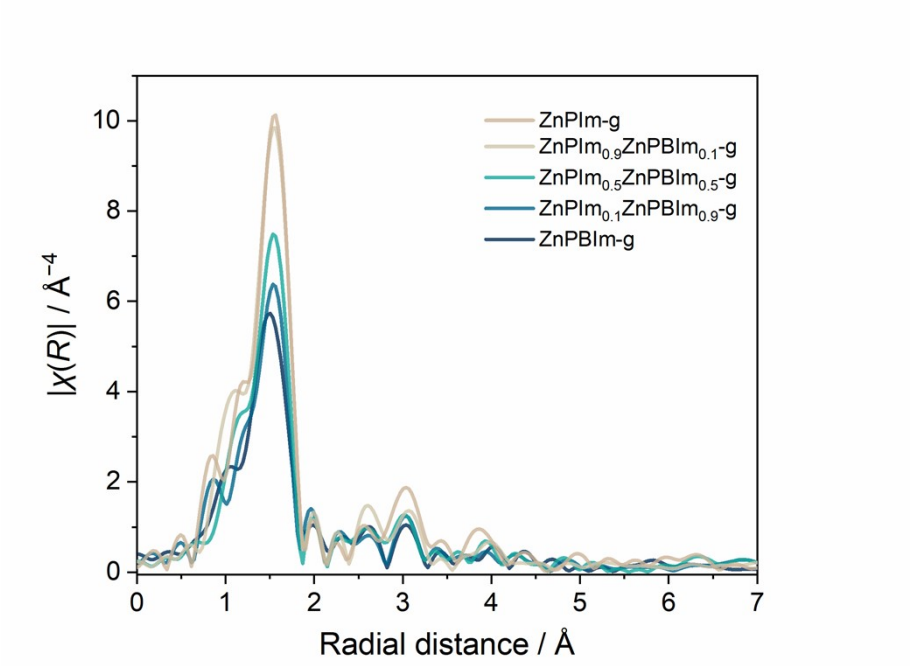

Fig. S30 Fourier transform extended X-ray absorption fine structure (EXAFS) at Zn K-edge of **$ZnPIm_{1-x}ZnPBIm_x$-g** where x = 0, 0.1, 0.5, 0.9, and 1.0.

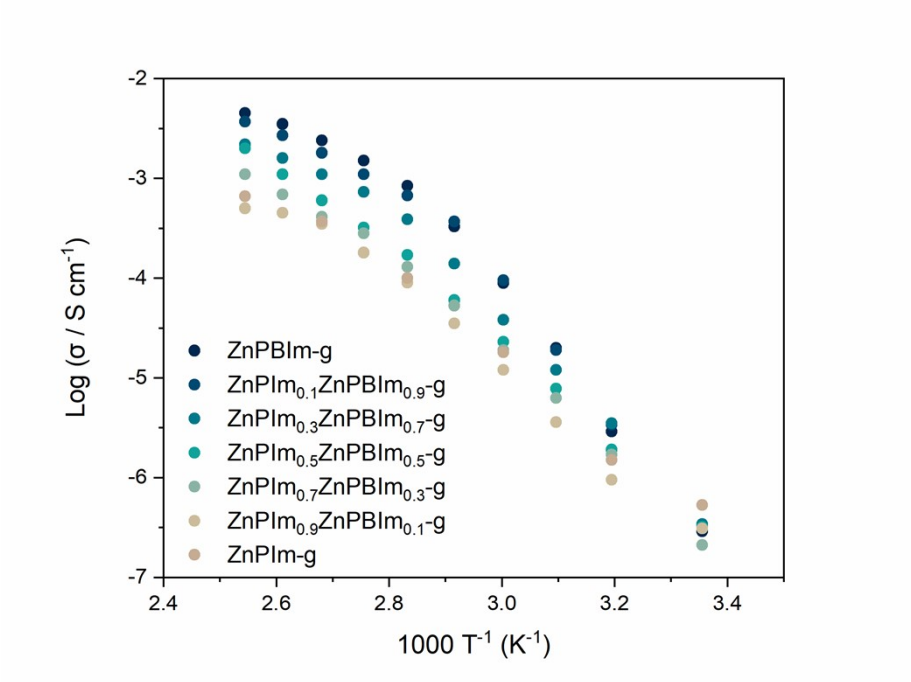

Fig. S31 Anhydrous H^+ conductivity of **$ZnPIm_{1-x}ZnPBIm_x$-g** where x = 0, 0.1, 0.5, 0.9, and 1.0.

Table S1. T_g and T_m of **$ZnPIm_{1-x}ZnPBIm_x$** where x = 0, 0.1, 0.5, 0.9, and 1.0.

	T_g / °C	T_m / °C	T_g/T_m
ZnPIm	10.8	158	0.66
$ZnPIm_{0.9}ZnPBIm_{0.1}$	11.9	151	0.67
$ZnPIm_{0.7}ZnPBIm_{0.3}$	16.4	160	0.67
$ZnPIm_{0.5}ZnPBIm_{0.5}$	20.7	148	0.70
$ZnPIm_{0.3}ZnPBIm_{0.7}$	22.1	164	0.68
$ZnPIm_{0.1}ZnPBIm_{0.9}$	25.4	136	0.73
ZnPBIm	26.2	161	0.69

Table S2. Viscosity reference temperature from ref 10.

Reference temperature	Viscosity / Pa·s
Practical melting temperature	≈1 to 10^1
Working point	10^3
Littleton softening point	$10^{6.6}$
Dilatometric softening temperature	10^8 to 10^9
Glass transformation temperature	≈$10^{11.3}$
Annealing point	10^{12} or $10^{12.4}$
Strain Point	$10^{13.5}$

3. References

1. S. Horike, D. Umeyama, M. Inukai, T. Itakura and S. Kitagawa, *J. Am. Chem. Soc.*, 2012, **134**, 7612–7615.
2. D. Umeyama, S. Horike, M. Inukai and S. Kitagawa, *J. Am. Chem. Soc.*, 2013, **135**, 11345–11350.
3. T. E. Faber and J. M. Ziman, *Philos. Mag.*, 1965, **11**, 153–173.
4. E. Lorch, *J. Phys. C: Solid State Phys.*, 1969, **2**, 229–237.
5. S. Kohara, M. Itou, K. Suzuya, Y. Inamura, Y. Sakurai, Y. Ohishi and M. Takata, *J. Phys. Condens. Matter.*, 2007, **19**, 506101.
6. K. I. Hadjiivanov, D. A. Panayotov, M. Y. Mihaylov, E. Z. Ivanova, K. K. Chakarova, S. M. Andonova and N. L. Drenchev, *Chem. Rev.*, 2020, **121**, 1286–1424.
7. d. N. D. Marcia Cordes and J. L. Walter, *Spectrochim. Acta, Part A*, 1968, **24**, 237–252.
8. S. Mohan, N. Sundaraganesan and J. Mink, *Spectrochim. Acta, Part A*, 1991, **47**, 1111–1115.
9. A. Suwaiyan, R. Zwarich and N. Baig, *J. Raman Spectrosc.*, 1990, **21**, 243–249.
10. J. E. Shelby, *Introduction to glass science and technology*, Royal Society of Chemistry, Cambridge, UK, 2nd edn., 2005.